



Experimental and numerical investigation on the behavior of strip footing on geocell reinforced sand

Muhammed Ghoneim^{1,2}, Mostafa El sawwaf², Ahmed Nasr²

¹*Civil Engineering Department, Faculty of Engineering, Delta University for Science and Technology, Gamasa, 11152, Egypt*

²*Structural Engineering Department, Faculty of Engineering, Tanta University, Tanta, Egypt*

Correspondence: [Muhammed Abd Elhady Ghoneim.]; [34517]; Tel [+201064667229];
Email : Mohamed.ghoneim@deltauniv.edu.eg
Email : mohammed138327@f-eng.tanta.edu.eg

ABSTRACT

Geosynthetic reinforcements have become increasingly popular in the last few years for usage in a variety of infrastructure projects because of their advantageous properties. One kind of geosynthetic that is produced as three-dimensional interconnected cells is called geocell. It can be used as a reinforcement to enhance base course behavior by offering lateral confinement, which increases the base course's stiffness and strength while lowering surface permanent deformation. Therefore, this research aims to study the behavior of strip footing rested on a geocell reinforced sand bed experimentally and numerically. In this research, a single geocell, filled with sand, was exposed to a vertical load until reaching failure. The testing process was modeled through the use of PLAXIS 3D numerical software. The effects of using a geocell as a reinforcement on load-bearing capacity and settlement at variable parameters, such as depth of placement, height, and length of reinforcement under axial compression load were studied. The results indicate that using geocell as soil reinforcement leads to a noticeable improvement in the bearing capacity and settlement response of the soil. The recommended geocell layer height, length, and placement depth that give the maximum bearing capacity improvement are presented and discussed. The effect of using geocell as soil reinforcement on the ultimate bearing capacity is estimated by bearing capacity ratio (BCR) and modulus of subgrade reaction (k_s).

Keywords: Soil reinforcement, Geocell, Geosynthetics, Strip footing, Numerical, Experimental.

1. Introduction

Geocell is one of the contemporary techniques for soil reinforcement in civil engineering projects. A polymeric cellular substance that resembles honeycomb is referred to as geocell. Soil confinement could be achieved by using the cellular network formed by these junctions that connect the cells. By enclosing the soil fully and offering all-around confinement, these geocells stop the soil from moving laterally. As a result, the soil-geocell layer distributes the load over a significantly wider region of the subgrade soil, acting as a rigid mat. This not only increases the foundation soil's total bearing capacity but also significantly reduces the soil's vertical and lateral deformations. Several laboratory investigations have been conducted to study the behavior of soil reinforced with geocells (Muthukumar et al., 2019; Pancar & Kumandaş, 2021; Pokharel et al., 2010; Shadmand et al., 2018; Sherin et al., 2017). A series of triaxial compression experiments using geocell reinforced soil samples were conducted by (Bathurst & Karpurapu, 1993; Chen et al., 2013; Rajagopal et al., 1999). The results indicated a minor variation in the friction angle values of specimens with and without geocell reinforcement. (Dash, Krishnaswamy, et al., 2001; Dash, Rajagopal, et al., 2001; Rajagopal et al., 1999) investigated the reinforced performance of geocell foundation mattress with varying cell sizes, infill material properties and loading conditions. They found that the effectiveness of the reinforcement depended not only on the adequate load transmission to the fill material (via friction and interlocking), but also on the stiffness of the reinforcement. The performance improvement increases with increase

in the width of the geocell layer up to $b=5D$ (D =diameter of the footing). (Yoon et al., 2008) conducted experimental study to investigate the geotechnical performance of waste tires for soil reinforcement from chamber tests. The findings indicated that the optimum embedment depth is $0.2B$. Improvement in bearing capacity is not observed when the embedment depth reaches $1B$. (Pokharel et al., 2009) investigated static and repeated loads on single-geocell reinforced bases. When compared to the unreinforced condition, it was shown that a single geocell's reinforcement reduced permanent deformation by about 1.5 times. (Tafreshi & Dawson, 2010) presented results from tests conducted on strip footings supported by geocell and planar reinforced sand beds with the similar properties as geotextile in a laboratory setting. The findings indicate that increasing reinforcement width, the number of planar layers, and geocell height all decreased reinforcing efficiency. (Latha & Murthy, 2007; Rajagopal et al., 1999) confirmed an increase in the stiffness and strength imparted by the confinement effect of geocell reinforcement. (Ram Rathan Lal & Mandal, 2014) studied experimentally the behavior of cellular-reinforced fly-ash walls under strip loading. They studied the effect of vertical spacing and dimensions of cellular reinforcement. The findings indicate that increasing the height and the coverage ratio of cellular reinforcement corresponded to a higher value of failure surcharge pressure. (Kargar & Mir Mohammad Hosseini, 2017) studied the influences of geocell height, width, pocket size and number of geocell layers on the bearing pressure- settlement behavior by employing a small-scale physical model. The results demonstrated that the ultimate bearing capacity increased from 1.6 to 7.1 times the capacity without reinforcement when the ratio of the geocell height to the plate width increased from 0.25 to 1.5. By extending the width of the geocell layer up to $5B$, significant increase in the bearing capacity and settlement of geocell reinforced sand is produced; after that, the improvement becomes minimal. (Shin et al., 2017) investigated the impact of the type of infill soils, together with the width, height, and shape of the geocell. They employed four distinct infill soils (silty, sandy, gravel, and weathered granite) on a silty soil foundation and conducted unreinforced and geocell reinforced tests. Compared to the unreinforced soil, the reinforced case had a load dispersion angle that was about 15% higher and earth pressure cell values that were around 50% to 60% lower. Numerous numerical investigations have been presented to study the behavior of soil reinforced with geocell (Adithan et al., 2021; Ari & Misir, 2021; Latha et al., 2009; Pratap et al., 2022; Sanjei & De Silva, 2016; Yang et al., 2010; Zidan, 2012). To evaluate the behavior of footings on geocells with additional basal geogrid-reinforced soil, comprehensive numerical and experimental studies were conducted by (Dash et al., 2003; A. M. Hegde & Sitharam, 2015; A. Hegde & Sitharam, 2013, 2015; Sireesh et al., 2009; Sitharam et al., 2005; Sitharam & Sireesh, 2006; Thallak et al., 2007). The results showed a significant enhancement in load-carrying capacity through the inclusion of a planar geogrid at the base of the geocell mattress. The research aims to study the effectiveness of using geocell as soil reinforcement on the bearing capacity and settlement response of the foundation, and to determine the optimal values for the variables. The effect of using geocell as soil reinforcement on the ultimate B. C. is estimated by bearing capacity ratio (BCR) and modulus of subgrade reaction (k_s). The ultimate bearing capacity of reinforced soil divided by the ultimate bearing capacity of unreinforced soil is known as the bearing capacity ratio (BCR). As for the value of (k_s) it is equal to the vertical stress divided by the corresponding settlement.

2. Laboratory model tests

2.1. Loading frame and test tank

A series of lab model tests were carried out using a test tank built of mild steel with interior dimensions of $1000*500*600$ mm. To enable a uniform leveling of the sand bed, The tank's interior faces were graduated at intervals of 50 mm. Steel angles were used to reinforce the tank's vertical edges in the middle and at the top of the sides. To prevent the effects of bulging, rigid battens are used as bracing, and a rigid steel beam serves as support. Figure 1. shows a schematic illustration of the test setup. To minimize friction between the tank sides walls and the soil, the tank's interior walls were polished to a smooth finish. In order to obtain the boundary conditions, the depth of the soil tank was increased up to $7b$, where b is the footing width, and $10b$ in the long direction, with the width of the tank equal the length of the strip footing. Moreover, to reduce the impact of box boundaries, the soil thickness was retained at least $5b$ below the strip footing.

2.2. Model footing

A steel strip footing with dimensions of $500*100*10$ mm was utilized. It had a hole in the top center to hold a ball bearing. The footing was placed on the sand substrate, its length matching the tank's breadth. A bearing ball transmits the load to the footing. This configuration generated a hinge. It permitted the footing to spin without restrictions while avoiding any moment transfer from the loading fixture.

2.3. Test material

2.3.1 Sand

The Unified Soil Classification System (USCS) classified the soil used in the test as poorly graded sand (SP). Table 1 provides the primary measured sand parameters and Fig. 2 illustrates the sand's grain size distribution. A series of direct shear tests was conducted on specimens with dimensions of 60 mm in length, 60 mm in width, and 40 mm in height, with a relative density of 60%. The tests were performed under normal loads of 25, 50, and 100 kPa. The calculated angle of internal friction was found to be 37°."

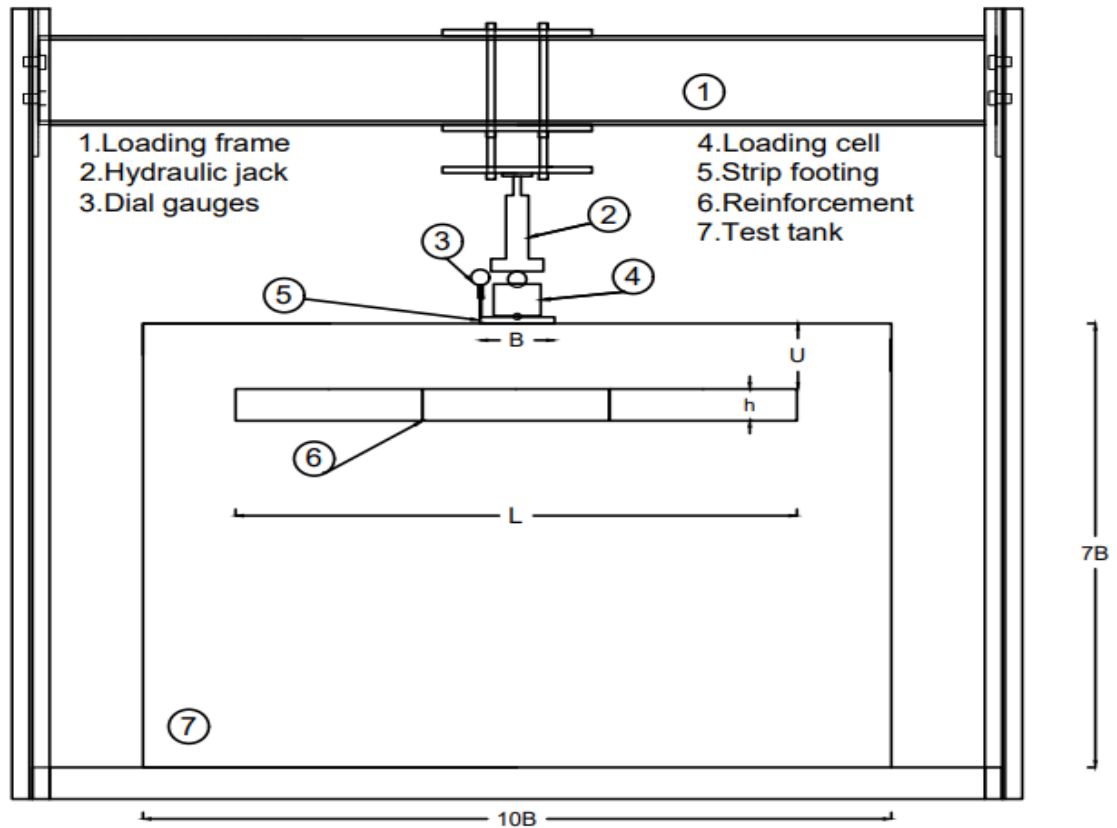


Fig. 1: Schematic diagram of model test

Table 1: The physical properties of the sand.

Properties	Value
Maximum dry unit weight, γ_{dmax} (Kn/m^3)	18.7
Minimum dry unit weight, γ_{dmin} (Kn/m^3)	15.8
O.M.C(%)	6.2
Specific gravity, G_s	2.633
The effective grain size, D_{10} (mm)	0.22
D_{30} (mm)	0.52
Mean grain size, D_{50} (mm)	0.68
D_{60} (mm)	0.77
Uniformity coefficient, C_u	3.53
Coefficient of curvature, C_c	1.6
Classification, USCS	SP
Maximum angle of internal friction, ϕ (degree)	44
Minimum angle of internal friction, ϕ (degree)	32.5
Maximum void ratio, e_{max} .	0.635
Minimum void ratio, e_{min} .	0.38
Sand at (Dr=60%)	
Dry unit weight, γ_{dry} (Kn/m^3)	17.45
Angle of internal friction, ϕ (degree)	37
Void ratio, e	0.48

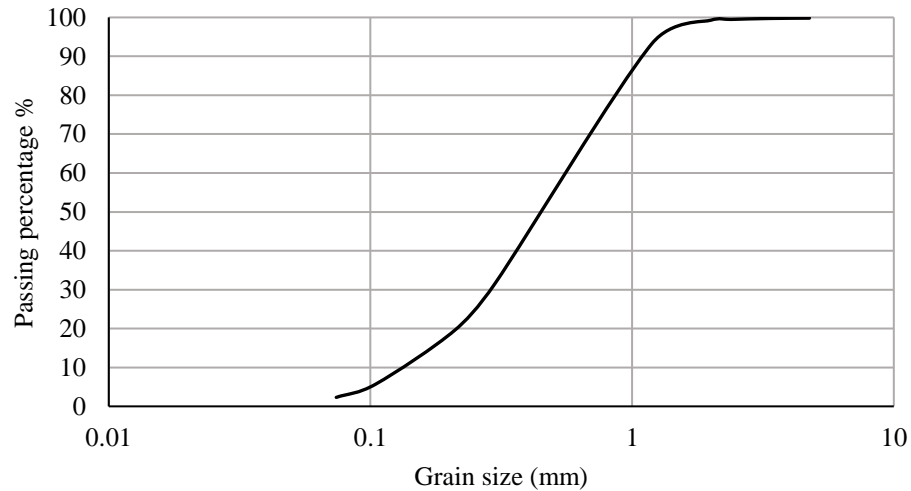


Fig. 2: The grain size distribution of the sand used.

2.3.2 Geocell

The perforated geocells have dimensions of 210 * 250 mm and are made of high-density polyethylene HDPE with a density of 0.95 g/cm³. The geometric shape of the geocell is illustrated in Fig. 3. The characteristics of geocell are summarized in Table 2. Figure 4 shows the stress-strain curve of the tensile test.

Table 2: The properties of geocell.

Properties	Value
Cell size (mm×mm)	250×210
Strip thickness (mm)	1.53
Density (g/cm ³)	0.95(±1.5%)
Tensile strength (Kn/m)	13.7



Fig. 3: The geometric shape of the geocell

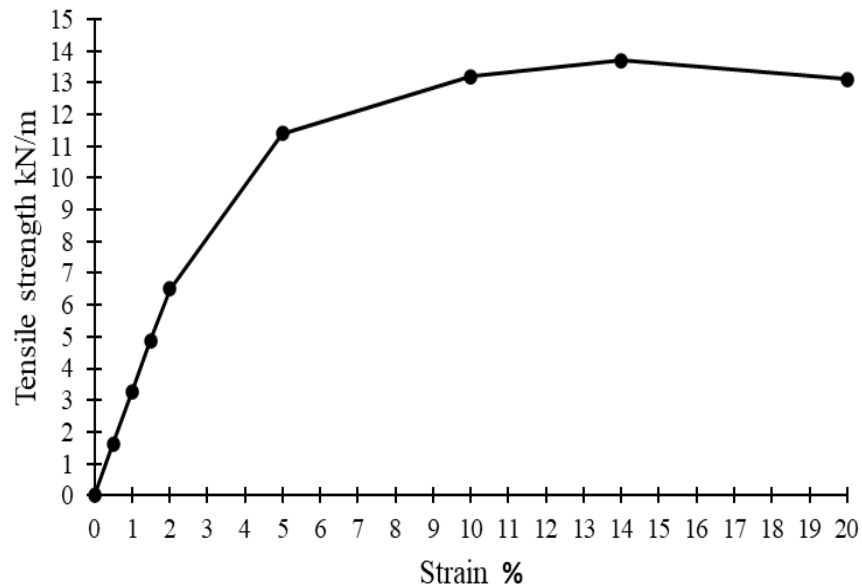


Fig. 4: Stress-strain curve of tensile test for geocell

2.4. *The experimental setup*

In the center of the tank, the footing was rested on top of the sand bed. A normal compressive load of 0.1 kN was applied to the model footing via a hydraulic jack supported on a reaction beam. Using a load cell, load increases were observed. Fig. 1 illustrates the loading setup. The settlement was determined by placing two dial gauges at each footing edge, and the average of the measurements was used to calculate the settlement in the center. To ensure that standard conditions were maintained throughout the investigations, each test required emptying and refilling the test tank. Sand was set in layers 50 mm thick. To regulate the unit weight of sand, the pre-calculated weight of sand was separately poured into the tank for each layer (50 mm). A straight piece of plywood was used to level the sand surface. A flat-bottom hammer (15 cm in diameter) weighing 20 N was used to achieve the required sand unit weight by compacting sand layers to the specified thickness. To monitor the achieved unit weight during tests, small cans with 40 mm in height and 40 mm in diameter were collected and placed at several locations in the tank. Following the tests, each individual weight can be measured and contrasted with the required unit weight of sand.

3. **Finite element modeling**

3.1. *Meshing and boundaries*

The finite element analysis software PLAXIS 3D V20 was used to analyze the numerical models used in this investigation. Figure 5 depicts the model's meshing and boundaries. The model's dimensions were selected to ensure that the distribution and values of the stresses and deformations are not influenced by the boundary distance. The displacement along the bottom boundary (which represents tank bottom) was restrained in both horizontal as well as vertical directions. The side boundaries (which represent tank side) were restrained only in the horizontal direction.

3.2. *Constitutive modeling*

In order to simulate the behavior of soil, the Mohr-Coulomb model was used. These basic soil parameters, which can be found using direct and triaxial shear measurements, serve as the foundation for this nonlinear model. The footing and reinforcement were modelled as a plate element. Table 3. depicts the characteristics of the material that were employed in the finite element analysis.

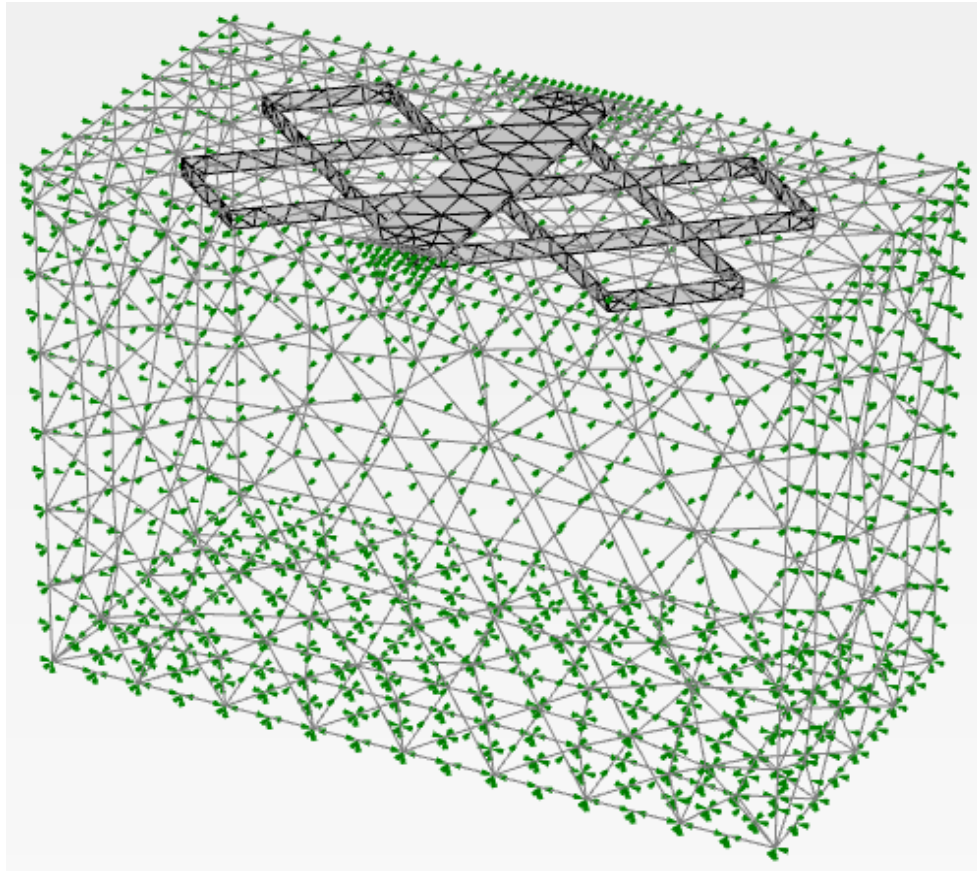


Fig. 5: Meshing and boundaries.

Table 3: Material properties

Parameter	Sand	Footing	Geocell
Material Model	Mohr-Column	Elastoplastic (Plate)	Elastoplastic (Plate)
Unit weight (kN/m ³)	17.45	74.5	9.5
Modules of Elasticity (KPa)	3300	207000000	220000
Poisson ratio	0.35	0.3	0.45
Angle of internal friction ϕ (degree)	37	-	-

3.3. Model Verification

Through comparing the vertical stress-settlement responses for various explored scenarios that were derived from the numerical study with the outcomes of the experimental analysis, PLAXIS was carried out. Figure 6 compares the findings of the current study with those of the experimental model. According to the figure, it can be concluded that the behavior of the experimental study is in good agreement with the numerical analysis results. Consequently, the behavior of geocells was successfully simulated in PLAXIS 3D models.

3.4. Parametric study

The bearing stress in relation to the settlement of the strip footing were studied with the variation of reinforcement length, height and placement depth as mentioned in Table 4. The findings were plotted to show how the researched parameters affected bearing capacity ratio (BCR) and the modulus of subgrade reaction k_s . The ultimate bearing capacity of reinforced soil divided by the ultimate bearing capacity of unreinforced soil is known as the bearing capacity ratio (BCR). As for the value of k_s it is equal to the vertical stress divided by the corresponding settlement.

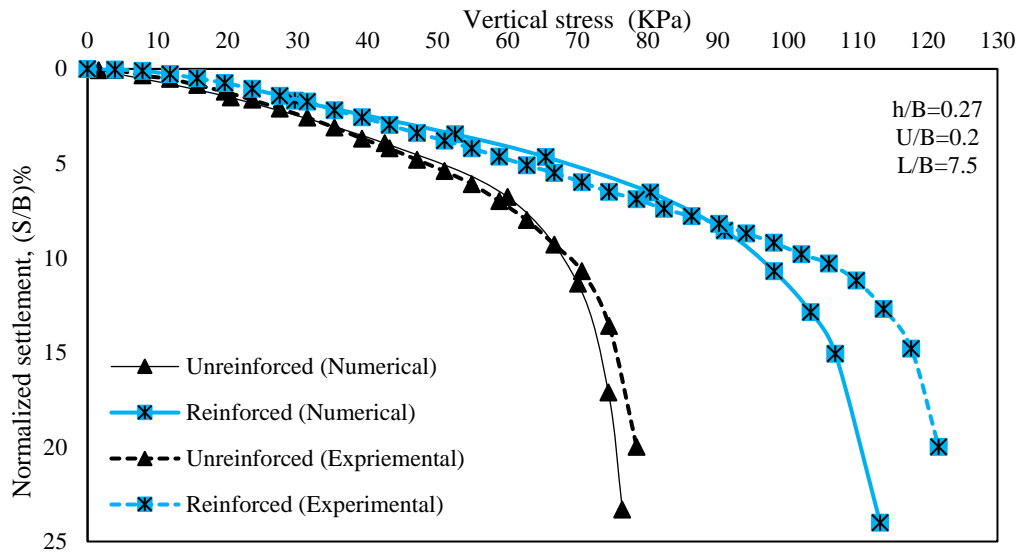


Fig. 6: Numerical and experimental results.

Table 4: Parametric analysis

Series	Test no.	Constant parameters	Variable parameter	
A	1	U=0.2B h =0.27B	Length of geocell layer (L)	
	2			2.5B
	3			5B
	4			7.5B
B	5	L=7.5B U=0.2B	Height of cell (h)	
	6			0.1B
	7			0.27B
	8			0.5B
	9			1B
C	10	L=7.5B h =0.27B	Depth of Placement(U)	
	11			0.1B
	12			0.2B
	13			0.3B
	14			0.4B
	15			0.5B
	16			0.8B

4. Results and discussion

4.1. Effect of Reinforcement Placement Depth (U)

It is possible to study the behavior of strip footing on sand through the results of tests gained from the relationship of displacement and vertical stress for different ratios such as placement depth ratio U/B, cell height ratio h/B and geocell layer length ratio L/B. Figure 7 shows the relationship between variation of vertical stress with normalized settlement for different placement depth ratios (U/B) at constant geocell layer length ratio L/B of 7.5 and constant geocell height ratio(h/B) of 0.27. The corresponding ultimate vertical stress were(85,104,100,95.3,91,80, and 75 KPa) for different placement depth ratios U/B of (0.1,0.2,0.3,0.4,0.5,0.8, and 1), respectively, while the value of the ultimate stress for the unreinforced case is 72 KPa.

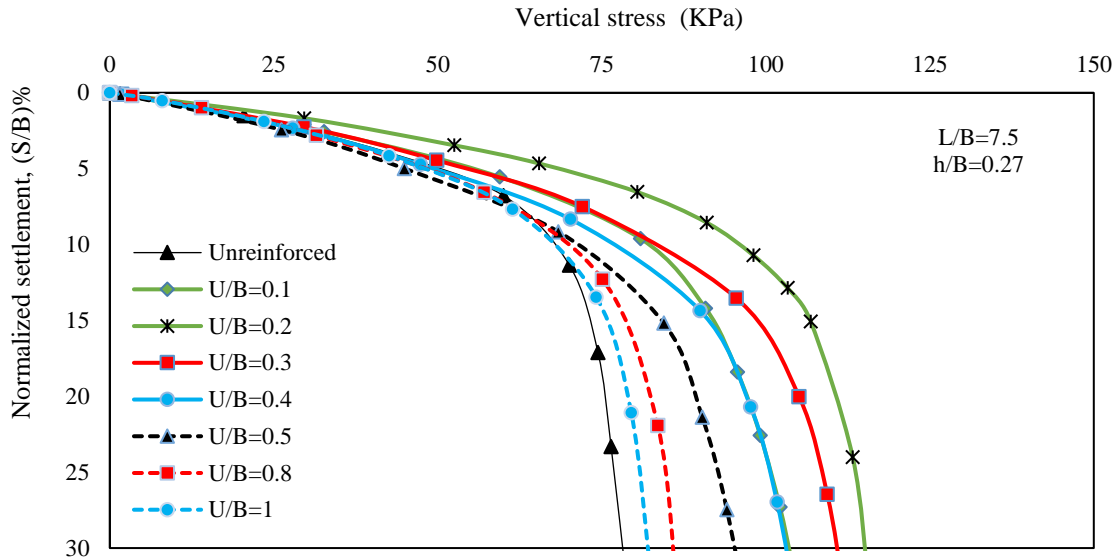


Fig. 7: Variation of vertical stress with normalized settlement for different placement depth.

Moreover, the displacement corresponding to the ultimate stress of unreinforced soil was 12 mm, where the values for reinforced case were (16.5,14,18,18,18,15, and 12 mm) for different placement depth ratios U/B of (0.1,0.2,0.3,0.4,0.5,0.8, and 1), respectively. From the results shown in Fig.8. It can be noted that the depth of placement reinforcement and the modulus of subgrade response k_s have a direct relationship. The figure clearly demonstrates that the modulus of subgrade reaction first rises with increasing depth until it reaches its greatest value, after which it falls with increasing placement depth of the geocell layer. The maximum improvement was obtained at depth ratio of U/B =0.2. The improvement in terms of bearing capacity ratio reaches to 1.44 as shown Fig.9. This can be explained by the observation that soil displacements under the footing are larger at shallow depths in both the horizontal and vertical directions. When reinforcement is placed at these depths, greater control is exerted over the lateral and vertical movements of the soil. Consequently, a significant improvement in the bearing capacity of the soil and its response to settlement is achieved. The zone between the footing and the geocell layer suffers more lateral and vertical soil displacements as geocell layer depth increases, which reduces the zone's bearing capacity. According to these findings, the top of the cell should be 0.2B below the bottom of the footing in order to receive the greatest benefit. The same result was recorded by (Yoon et al., 2008).

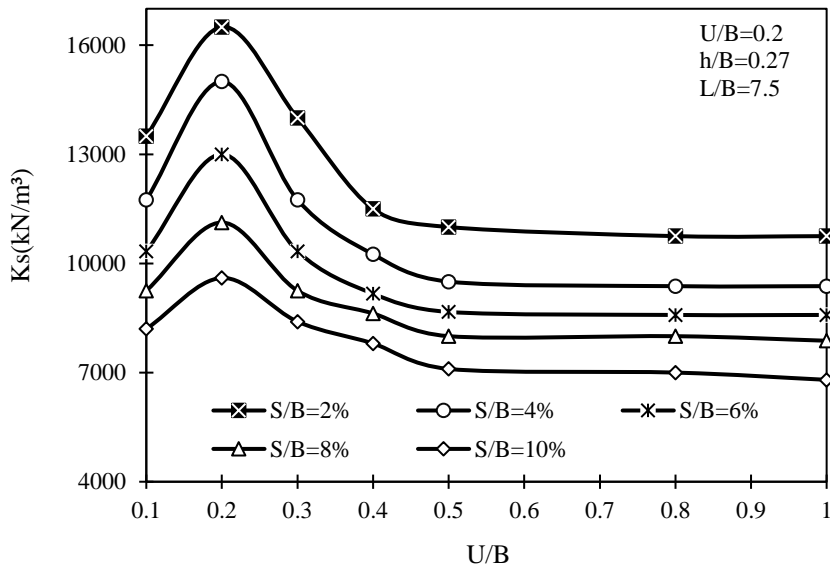


Fig.8: Variation of modules of subgrade reaction with normalized placement depth.

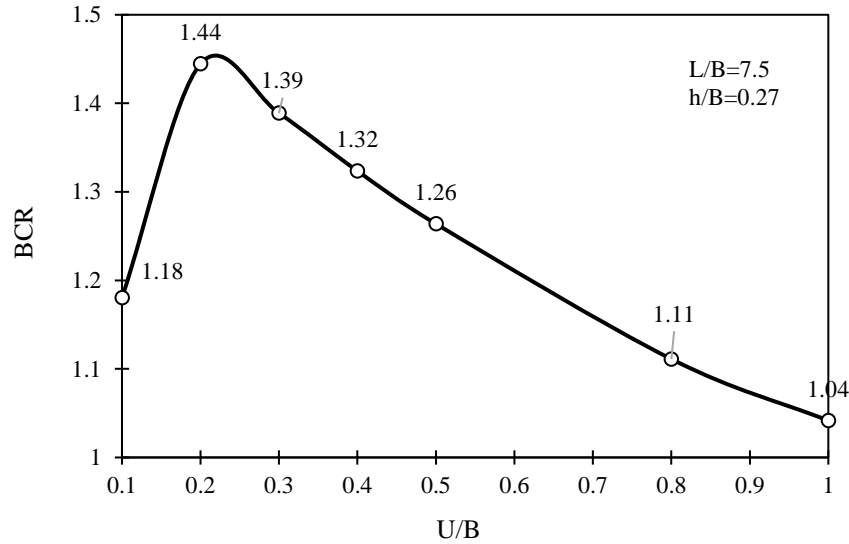


Fig.9: Variation of bearing capacity ratio with normalized placement depth.

4.2. Effect of cell height (h)

Figure 10 shows the relationship between variation of vertical stress with normalized settlement for different height ratios (h/B) at constant geocell layer length ratio L/B of 7.5 and constant geocell layer placement depth ratio U/B of 0.2. The corresponding ultimate vertical stress were (80,104,126,186, and KPa) for different heights ratios (h/B) of (0.1,0.27,0.5,1, and 2), respectively, the displacement corresponding to the ultimate stress of reinforced case were (13.3,14,16.4,19.2 and 22mm) for different heights ratios (h/B) (0.1,0.27,0.5,1, and 2), respectively.

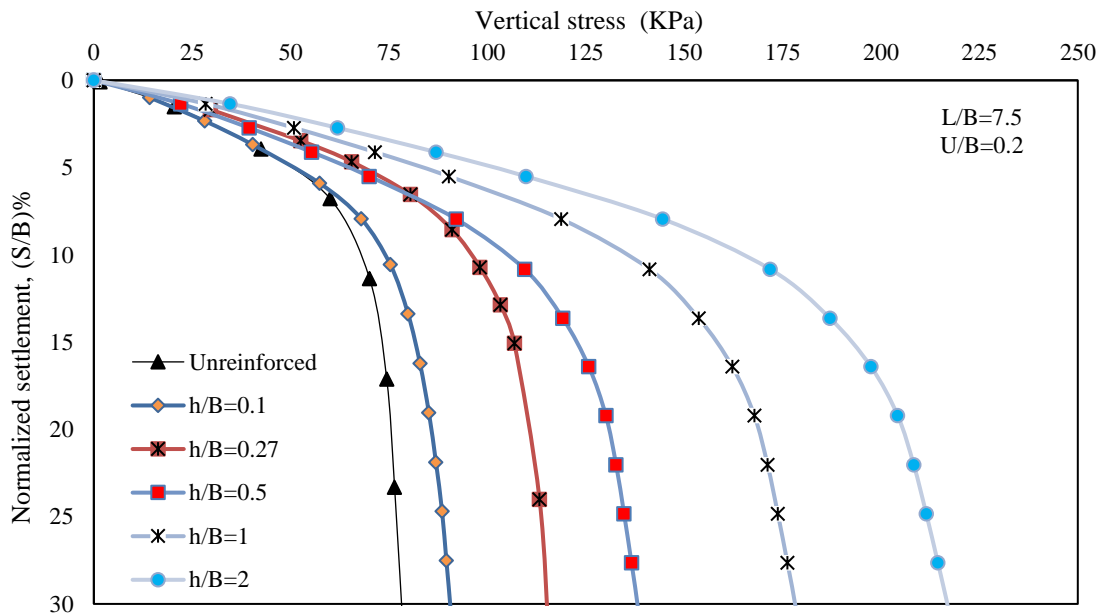


Fig. 10: Variation of vertical stress with normalized settlement for different cell height.

Five different heights were used in the studies to examine the impact of cell height on the footing behavior. The variation of modules of subgrade reaction with cell height ratio h/B is shown in Fig.11. The figure demonstrates that raising cell height leads to improved subgrade reaction modules. The soil in the geocell pocket beneath the footing has a tendency to press down into the subgrade upon loading by overcoming friction on the geocell wall. Since the surface area has risen, the overall frictional resistance on the geocell walls increases as the height of the

geocell rises. Consequently, the entire geocell mattress exhibits composite body behavior, improving performance. Additionally, as the cell's height increases, the geocell mattress's moment of inertia and its bending and shear rigidity increase. This redistributes the footing pressure over a wider area, improving the footing's performance. The corresponding bearing capacity ratio was (1.11,1.44,1.75,2.33, and 2.89) for different heights ratios (h/B) of (0.1,0.27,0.5,1, and 2), respectively as shown in Fig.12.

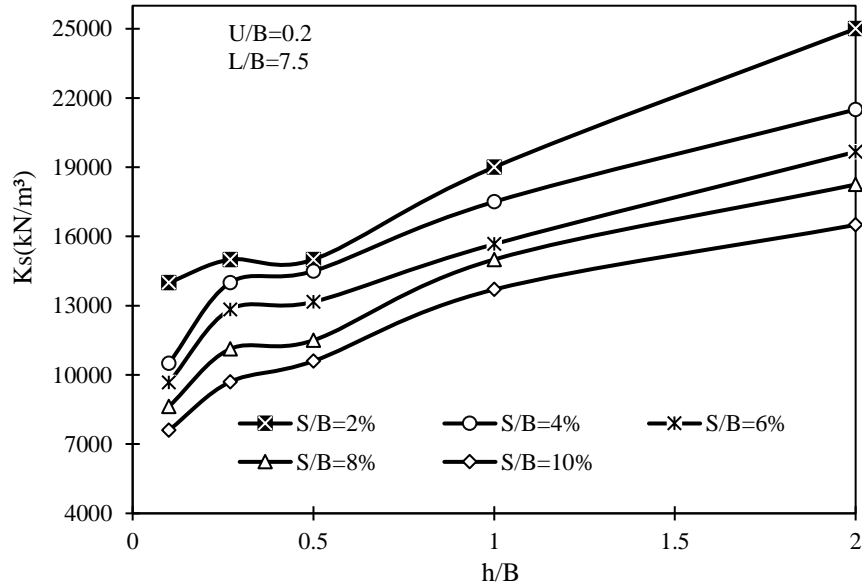


Fig.11: Variation of modules of subgrade reaction with normalized reinforcement height.

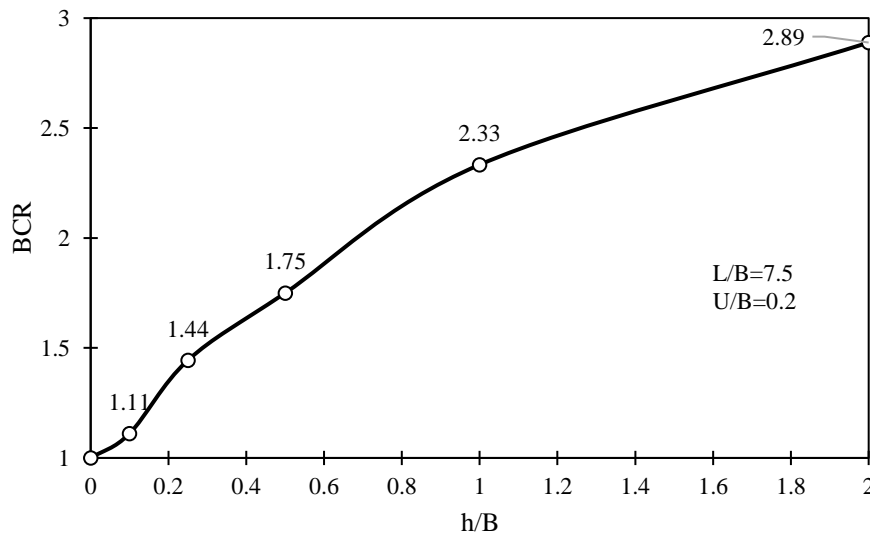


Fig.12: Variation of bearing capacity ratio with normalized reinforcement height.

4.3. Effect of geocell layer length (L)

Figure 13 shows the relationship between variation of vertical stress with normalized settlement for different Length ratios (L/B) at constant geocell layer placement depth ratio U/B of 0.2 and constant geocell height ratio(h/B) of 0.27. The corresponding ultimate vertical stress were(85,98,104, and 106 KPa) for different Length ratios (L/B) of (2.5,5,7.5and 10), respectively, the displacement corresponding to the ultimate stress of reinforced case were (17.25,18,14 and 14.5mm) for different Length ratios (L/B) of (2.5,5,7.5and 10), respectively.

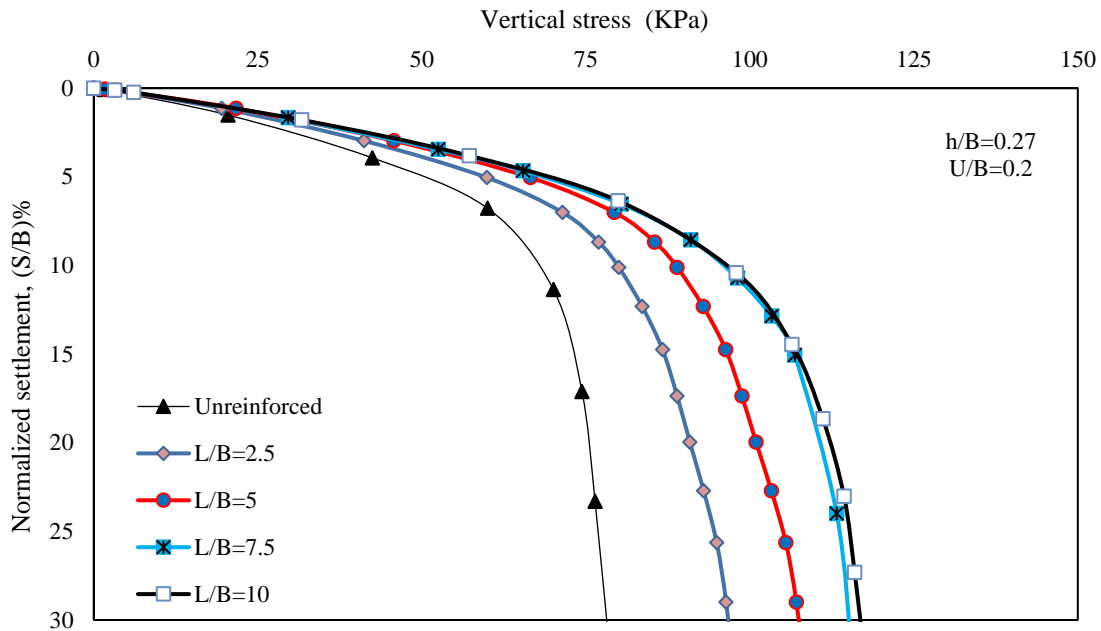


Fig. 13: Variation of vertical stress with normalized settlement for different reinforcement length.

From the results shown in Fig.14. it can be stated that there is a direct relationship between the improvement in the modulus of subgrade reaction k_s and the length of the reinforcement, caused by the confinement and friction effect provided by the geocell walls to the sand trapped inside them, which behaves as a relatively rigid member, and increases the bearing capacity. Fig.15. shows the relation between the bearing capacity ratio with normalized reinforcement length. The optimum length of reinforcement is 7.5 B, at which the value of the enhancement in bearing capacity ratio is significantly tangible, and any increase after this length leads to an insignificant improvement.

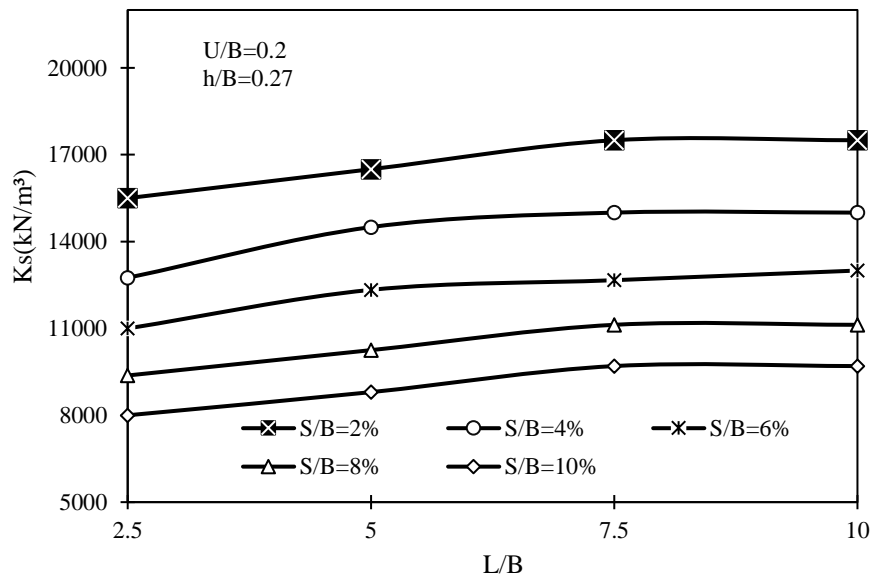


Fig.14: Variation of modules of subgrade reaction with normalized reinforcement length.

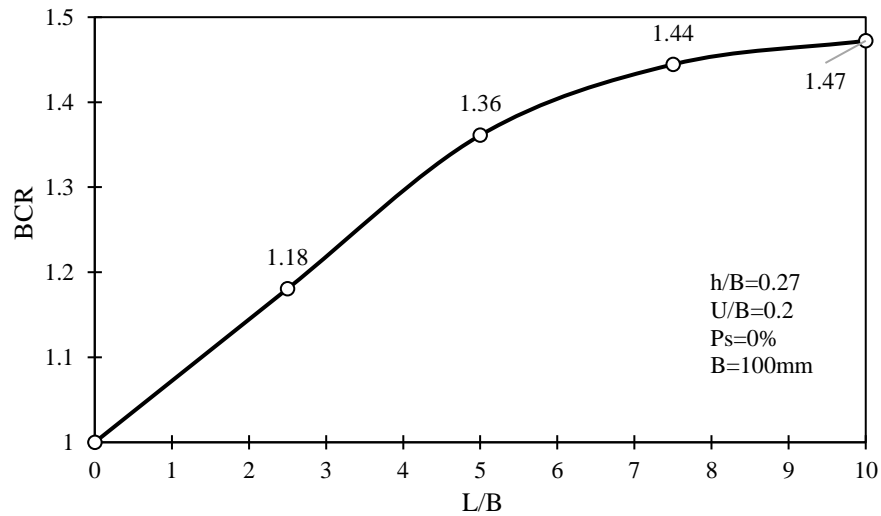


Fig.15: Variation of bearing capacity ratio with normalized reinforcement length.

Conclusion

- 1- The geocell-reinforced sand offers lateral and vertical confinement, a tensioned membrane effect, and a larger stress distribution when compared to unreinforced sand. This results in a considerable improvement in load bearing capacity and decreasing in settlement response.
- 2- The ideal depth for placing geocell reinforcement is roughly $U = 0.2$ times the width of the footing. Any increase in placement depth u beyond $U = 0.2B$ results in a decrease in the improvement of bearing capacity. It is observed that when reaching a placement depth equal to $U = 1B$ there is no significant improvement in bearing capacity.
- 3- The optimal length for geocell reinforcement (L) falls within the range of 5 to 7.5 times the width of the footing. Any extension of the reinforcement layer length beyond $L = 7.5B$ leads to a negligible increase.
- 4- The increased height of the geocell layer provides an increased moment of inertia and improved bending and shear rigidity for the geocell mattress. These improvements in the geocell mattress redistribute the footing pressure over a wider area, improving the overall performance of the footing.
- 5- The percentage of improvement in bearing capacity in the case of soil reinforced with geocells at placement depth (U) = $0.2B$, length $L = 7.5B$, and height $h = 0.27B$ is equal 44% and increases significantly with increasing cell height. The percentage of improvement in bearing capacity in the case of cell with height of $h = 2B$ is equal 189%.

Disclosure

The author reports no conflicts of interest in this work.

References

- Adithan, K., Chandra, A. C. N., Reddy, T. L. G., Vignesh, G. V., Sharma, A., & Ramkrishnan, R. (2021). Numerical Analysis of Soil Reinforcement using Geocell infilled with Quarry Dust Powder. *Journal of Physics: Conference Series*, 2070(1), 012189.
- Ari, A., & Misir, G. (2021). Three-dimensional numerical analysis of geocell reinforced shell foundations. *Geotextiles and Geomembranes*, 49(4), 963–975. <https://doi.org/10.1016/j.geotexmem.2021.01.006>
- Bathurst, R. J., & Karpurapu, R. (1993). Large-Scale Triaxial Compression Testing of Geocell-Reinforced Granular Soils. *Geotechnical Testing Journal*, 296–303.
- Chen, R.-H., Huang, Y.-W., & Huang, F.-C. (2013). Confinement effect of geocells on sand samples under triaxial compression. *Geotextiles and Geomembranes*, 37, 35–44.
- Dash, S. K., Krishnaswamy, N. R., & Rajagopal, K. (2001). Bearing capacity of strip footings supported on geocell-reinforced sand. *Geotextiles and Geomembranes*, 19(4), 235–256.
- Dash, S. K., Rajagopal, K., & Krishnaswamy, N. R. (2001). Strip footing on geocell reinforced sand beds with additional planar reinforcement. In *Geotextiles and Geomembranes* (Vol. 19).
- Dash, S. K., Sireesh, S., & Sitharam, T. G. (2003). Model studies on circular footing supported on geocell reinforced sand underlain by soft clay. *Geotextiles and Geomembranes*, 21(4), 197–219.
- Hegde, A. M., & Sitharam, T. G. (2015). Three-dimensional numerical analysis of geocell-reinforced soft clay beds by considering the actual geometry of geocell pockets. *Canadian Geotechnical Journal*, 52(9), 1396–1407.
- Hegde, A., & Sitharam, T. G. (2013). Experimental and numerical studies on footings supported on geocell reinforced sand and clay beds. *International Journal of Geotechnical Engineering*, 7(4), 346–354. <https://doi.org/10.1179/1938636213Z.00000000043>
- Hegde, A., & Sitharam, T. G. (2015). 3-Dimensional numerical modelling of geocell reinforced sand beds. *Geotextiles and Geomembranes*, 43(2), 171–181. <https://doi.org/10.1016/j.geotexmem.2014.11.009>
- Kargar, M., & Mir Mohammad Hosseini, S. M. (2017). Effect of reinforcement geometry on the performance of a reduced-scale strip footing model supported on geocell reinforced sand. *Scientia Iranica*, 24(1), 96–109.
- Latha, G. M., Dash, S. K., & Rajagopal, K. (2009). Numerical simulation of the behavior of geocell reinforced sand in foundations. *International Journal of Geomechanics*, 9(4), 143–152.
- Latha, G. M., & Murthy, V. S. (2007). Effects of reinforcement form on the behavior of geosynthetic reinforced sand. *Geotextiles and Geomembranes*, 25(1), 23–32.
- Muthukumar, S., Sakthivelu, A., Shanmugasundaram, K., Mahendran, N., & Ravichandran, V. (2019). Performance assessment of square footing on jute geocell-reinforced sand. *International Journal of Geosynthetics and Ground Engineering*, 5, 1–10.
- Pancar, E. B., & Kumandaş, A. (2021). The Effects of Geocell Height and Lime Stabilization on Unpaved Road Settlements at Different Water Contents. *Advances in Civil Engineering*, 2021.
- Pokharel, S. K., Han, J., Leshchinsky, D., Parsons, R. L., & Halahmi, I. (2009). Behavior of geocell-reinforced granular bases under static and repeated loads. In *Contemporary topics in ground modification, problem soils, and geo-support* (pp. 409–416).
- Pokharel, S. K., Han, J., Leshchinsky, D., Parsons, R. L., & Halahmi, I. (2010). Investigation of factors influencing behavior of single geocell-reinforced bases under static loading. *Geotextiles and Geomembranes*, 28(6), 570–578. <https://doi.org/10.1016/j.geotexmem.2010.06.002>
- Pratap, U., Azhar, M., & Choudhary, A. K. (2022). Numerical analysis of geocell-reinforced embankment using PLAXIS 3D. *Advances in Geo-Science and Geo-Structures: Select Proceedings of GSGS 2020*, 283–292.
- Rajagopal, K., Krishnaswamy, N. R., & Latha, G. M. (1999). Behaviour of sand confined with single and multiple geocells. *Geotextiles and Geomembranes*, 17(3), 171–184.
- Ram Rathan Lal, B., & Mandal, J. N. (2014). Behavior of cellular-reinforced fly-ash walls under strip loading. *Journal of Hazardous, Toxic, and Radioactive Waste*, 18(1), 45–55.

- Sanjei, C., & De Silva, L. I. N. (2016). Numerical modelling of the behaviour of model shallow foundations on geocell reinforced sand. *2016 Moratuwa Engineering Research Conference (MERCon)*, 216–221.
- Shadmam, A., Ghazavi, M., & Ganjian, N. (2018). Load-settlement characteristics of large-scale square footing on sand reinforced with opening geocell reinforcement. *Geotextiles and Geomembranes*, 46(3), 319–326. <https://doi.org/10.1016/j.geotexmem.2018.01.001>
- Sherin, K. S., Chandrakaran, S., & Sankar, N. (2017). Effect of Geocell Geometry and Multi-layer System on the Performance of Geocell Reinforced Sand Under a Square Footing. *International Journal of Geosynthetics and Ground Engineering*, 3(3). <https://doi.org/10.1007/s40891-017-0097-3>
- Shin, E. C., Kang, H. H., & Park, J. J. (2017). Reinforcement efficiency of bearing capacity with geocell shape and filling materials. *KSCE Journal of Civil Engineering*, 21(5), 1648–1656. <https://doi.org/10.1007/s12205-016-1649-0>
- Sireesh, S., Sitharam, T. G., & Dash, S. K. (2009). Bearing capacity of circular footing on geocell–sand mattress overlying clay bed with void. *Geotextiles and Geomembranes*, 27(2), 89–98.
- Sitharam, T. G., & Sireesh, S. (2006). Effects of base geogrid on geocell-reinforced foundation beds. *Geomechanics and Geoengineering: An International Journal*, 1(3), 207–216.
- Sitharam, T. G., Sireesh, S., & Dash, S. K. (2005). Model studies of a circular footing supported on geocell-reinforced clay. *Canadian Geotechnical Journal*, 42(2), 693–703.
- Tafreshi, S. N. M., & Dawson, A. R. (2010). Comparison of bearing capacity of a strip footing on sand with geocell and with planar forms of geotextile reinforcement. *Geotextiles and Geomembranes*, 28(1), 72–84. <https://doi.org/10.1016/j.geotexmem.2009.09.003>
- Thallak, S. G., Saride, S., & Dash, S. K. (2007). Performance of surface footing on geocell-reinforced soft clay beds. *Geotechnical and Geological Engineering*, 25(5), 509–524.
- Yang, X., Han, J., Parsons, R. L., & Leshchinsky, D. (2010). Three-dimensional numerical modeling of single geocell-reinforced sand. *Frontiers of Architecture and Civil Engineering in China*, 4(2), 233–240. <https://doi.org/10.1007/s11709-010-0020-7>
- Yoon, Y. W., Heo, S. B., & Kim, K. S. (2008). Geotechnical performance of waste tires for soil reinforcement from chamber tests. *Geotextiles and Geomembranes*, 26(1), 100–107.
- Zidan, A. F. (2012). Numerical study of behavior of circular footing on geogrid-reinforced sand under static and dynamic loading. *Geotechnical and Geological Engineering*, 30(2), 499–510.